JOURNAL OF AIRCRAFT
Vol. 34, No. 4, July–August 1997

Direct Calculation of Three-Dimensional Indicial Lift Response Using Computational Fluid Dynamics

Rajneesh Singh* and James D. Baeder†
University of Maryland, College Park, Maryland 20742

An unsteady Euler solver is modified to calculate the indicial response of a rectangular wing to a step change in the angle of attack. In this new approach the grid time metrics include the velocity caused by the impulsive change in angle of attack, but the mesh is not moved accordingly. This approach avoids numerical instabilities and decouples the step change in the angle of attack from a pitch rate. Numerical results are validated by comparison with analytical results for two-dimensional indicial responses. The application of the same method to rectangular wings reveals important characteristics of the three-dimensional indicial response. It is found that the direct calculation of the indicial response using computational fluid dynamics gives quite accurate results and provides a rich database, in the absence of experimental data, to validate the approximations to indicial response.

Introduction

THE indicial lift response is the response of a wing to a step change in a forcing parameter, such as angle of attack or pitch rate. Determination of the indicial response to a step change in the angle of attack is very important; it forms the basis for calculating the response to an arbitrary motion. With the increasing use of computational fluid dynamics (CFD) in the design stages of airvehicle development, it is necessary for CFD codes to be able to simulate aerodynamic flowfields in all expected flight conditions. Presently, however, the full simulation of unsteady flowfields is not practical for routine calculations because of the enormously large computational resources required. In such cases, the aerodynamic loads can be efficiently and quite accurately estimated by using approximations of the indicial functions. The airloads resulting from an arbitrary change in the angle of attack are calculated by superposition of indicial solutions having different elapsed time since the beginning of the motion. Use of indicial formulations to determine the unsteady aerodynamics loads is several orders of magnitude faster than Euler codes. However, the accuracy of the indicial response determination affects the prediction of unsteady aerodynamic loads. The accuracy of both the magnitude and the phase with respect to the change in the angle of attack is important for the analysis of aeroelastic problems.

Unfortunately, indicial responses can be determined analytically for all time only for two-dimensional airfoils in incompressible and inviscid flows.[1] The effects of compressibility can be rigorously included only for short periods[2]; whereas three dimensionality of the flow does not allow for an analytical determination of the indicial lift response of a wing. Rather, one has to use approximate functions to represent the indicial lift responses for practical applications.[3–4]

The main objective of the present study is to directly calculate the indicial response of a wing to a step change in the angle of attack. The numerical database generated for various Mach numbers for wings of different aspect ratios can be used to develop and validate approximation functions for the indicial response. The role of three-dimensional effects is examined to explore the possibilities of expressing approximate indicial response function for wings of different aspect ratios. The lift histories and pressure contours are examined to study and explain the characteristics of the indicial response.

Received Aug. 7, 1996; revision received Feb. 24, 1997; accepted for publication Feb. 27, 1997.

*Research Assistant, Alfred Gessow Rotorcraft Center, Department of Aerospace Engineering. Student Member AIAA.

†Assistant Professor, Alfred Gessow Rotorcraft Center, Department of Aerospace Engineering. Senior Member AIAA.

Indicial Theory

An indicial response to a step change in the angle of attack consists of two distinct regions, each having different flow physics, with an intermediate overlapping region. In the frequency domain these are the responses in the low (steady) and the high-frequency limits. The initial part of the response arises because of the impulsive motion of the body and the resulting pressure difference on the upper and the lower surface of the wing. As the body moves impulsively, a pressure differential is created that is caused by a compression wave on the upwind surface and an expansion wave on the other. Assuming linear compressible flow, the magnitude of the pressure difference is uniform across the chord and depends only on the Mach number. This initial loading is the noncirculatory loading. The noncirculatory loading decays rapidly from the initial value within a few chord lengths of the distance traveled. This loading can be computed directly for two-dimensional subsonic and supersonic flow quite accurately using linear piston theory. The initial value of the lift magnitude as given by linear piston theory is:

$$C_L(T = 0) = (4/M)\Delta\alpha$$

where M is the freestream Mach number and $\Delta\alpha$ is the step change in the angle of attack.

The second part of the response is related to the steady-state response to the effective angle of attack caused by the step input. This part is called the circulatory response and it is asymptotically reached after the perturbation caused by the noncirculatory loading has decayed. This part can be determined accurately using quasisteady theory. The final value of the lift as given by linearized quasisteady theory is

$$C_L(T \to \infty) = (2\pi/\sqrt{1 - M^2})\Delta\alpha$$

The main problem in the determination of the indicial response is calculating the response in the intermediate overlapping region. The flow is highly unsteady and little is known about the development of the flow from the initial input to the final steady state. Lomax[2] obtained the indicial response for a flat

plate in linearized compressible flow for small time using numerical integration. The usual approach for the compressible indicial response determination is to make use of semi-empirical methods,[4] whereby experimental results are used in conjunction with the linear subsonic aerodynamic theory to arrive at the best possible approximation. Important parameters in forming the approximate functions are the initial lift magnitude and the time derivative of the lift at $T = 0$ and the steady-state lift magnitude. Unfortunately, accurate experimental results are difficult to get because of practical problems associated in giving step input in an experimental setup. However, it is possible to relate experiments for oscillating flows back to the indicial response from the frequency domain.[4]

Because of the lack of purely analytical methods for three-dimensional compressible flows, CFD methods can be effectively used to determine the indicial response. One of the advantages with the use of CFD methods is that the pressure history can be obtained over the entire flow domain. This not only gives the information about the unsteady loading, but provides important insight into the flow development. The main problem in using CFD methods is the numerical instabilities that may arise if the step change in the angle of attack is not incorporated judiciously. This problem has been avoided in the past by indirect computation of the indicial response.[5] Instead of calculating response to the step change, a smoothly varying input is used and the response to the step input is calculated by mathematical transformations. However, it is difficult to remove effects of the pitch rate on the solution inherent in this approach. Such methods also do not provide information about the development of the flow. A better use of the power of CFD methods can be made in direct calculation of the indicial response.

CFD Methodology

Governing Equations

The Euler equations were chosen to study the aerodynamic response of the wing to a step change in the angle of attack. The Euler equations were chosen since they are able to handle the possibly strong nonlinear shocks at transonic Mach numbers (as compared to the Potential equation) while being computationally efficient (as compared to the Navier–Stokes equations and the resulting fine mesh). Since the aerodynamic quantity of interest in this study is the lift coefficient, the effect of viscous forces is expected to be unimportant.

Algorithm

The Transonic Unsteady Rotor Navier–Stokes (TURNS) code[6] has been applied to a variety of helicopter aerodynamic and acoustic problems. The TURNS code uses Roe upwinding with higher-order MUSCL-type limiting on the right-hand side for spatial accuracy. A lower–upper symmetric Gauss–Seidel (LU–SGS) implicit operator is used on the left-hand side to increase stability and robustness. Unfortunately, the use of a spectral radius approximation in the implicit scheme renders the method only first-order accurate in time. Therefore, in this study a second-order backwards difference in time is used along with Newton-type subiterations to restore formal second-order time accuracy. This also reduces the factorization and linearization errors associated with the scheme. In the present study viscous effects are ignored and the code is only used in Euler mode.

Incorporation of Indicial Step Change

In this study a new approach, called a field velocity approach, is used to calculate the indicial response. The field velocity approach can be considered as an extension of the surface transpiration approach. The velocity correction is applied throughout the flowfield as opposed to only on the surface as in the surface transpiration method. An impulsive change in the angle of attack can be perceived as an impulsive superposition of a uniform velocity field normal to the freestream. The magnitude of the normal velocity is determined by the magnitude of the indicial angle-of-attack change. This superposed velocity field is modeled by modifying the grid time metrics. However, the grid is not actually distorted because of the modified time metrics. This is similar to quasi-steady calculations, where grid time metrics are calculated, but the mesh is not actually moved. Mathematically, the field velocity approach can be explained by considering the velocity field $\boldsymbol{V}$ in the computational domain. It can be written as

$$\boldsymbol{V} = (u - x_\tau)\boldsymbol{i} + (v - y_\tau)\boldsymbol{j} + (w - z_\tau)\boldsymbol{k}$$

where u, v, and w are the components of the velocity along the coordinate directions and x_τ, y_τ, and z_τ are the grid time metrics components. For the flow over a stationary wing these components are zero. Let an indicial change in the angle of attack be represented by velocity w^i along the z direction. Thus, the velocity field becomes

$$\boldsymbol{V} = (u - x_\tau)\boldsymbol{i} + (v - y_\tau)\boldsymbol{j} + (w - z_\tau + w^i)\boldsymbol{k}$$

The field velocity approach models this changed velocity field by modifying the time metrics. The modified time metrics are defined as

$$\tilde{x}_\tau\boldsymbol{i} + \tilde{y}_\tau\boldsymbol{j} + \tilde{z}_\tau\boldsymbol{k} = x_\tau\boldsymbol{i} + y_\tau\boldsymbol{j} + (z_\tau - w^i)\boldsymbol{k}$$

This simple velocity correction approach, besides being free of numerical oscillations, also provides a way to determine the response resulting from a pure step change in the angle of attack without any accompanying pitch rate term. The accuracy of the method is validated by comparing numerical results for a two-dimensional airfoil with the exact linear analytical results for a flat plate. This same approach can be applied to a stationary gust problem[7] or to incorporate the complicated three-dimensional wake of a rotor blade.[8]

Mesh Geometry

The indicial responses of a wing are calculated at Mach numbers of 0.3, 0.5, and 0.8 for a step change of 2 deg in the angle of attack (results are nearly identical for a step change of 3 deg in the angle of attack). This encompasses the range from low subsonic to transonic flows. Untwisted wings of rectangular planform with a NACA 0012 airfoil cross section are chosen for this study. To examine the effects of tip relief, two different aspect ratios are examined: 5 and 10. Although more complex geometries can be modeled using CFD, this simple geometry was chosen to demonstrate the similarities and differences with two-dimensional flow.

The three-dimensional calculations for the wing with an aspect ratio of 5 are performed on a C–H mesh with 181 points in the wrap around direction (133 points on the surface), 34 points in the spanwise direction (25 points on the surface), and 31 points in the normal direction. The computational domain extends approximately 10 chords in the normal direction and 4 chords outboard from the tip in the spanwise direction. Additional spanwise stations are added inboard for the calculations for a wing with an aspect ratio of 10. Thus, the two meshes are identical for the outboard five chords. This is important in comparing the results from the two wings with different aspect ratios at equal chord distances from the tip.

A steady-state solution at 0 deg angle of attack is obtained for each case. Then, unsteady calculations are performed for a step change in the angle of attack of 2 deg. A nondimensional time step size, based on the freestream speed of sound and the chord of the wing, of 0.05 along with five Newton-like subiterations is used to advance the solution in time. For these parameters numerical results were similar for a finer mesh and for smaller time step sizes.

To validate the accuracy of the method, two-dimensional indicial responses are also calculated for a NACA 0006 airfoil using 181 × 31 grid points (the same mesh size as for one spanwise station of the wings). Since the analytical results are possible only for the flat plate, the 6% thickness ratio was chosen to reduce the effects of thickness on the lift response.

Two-Dimensional Validation with Theory

Typical indicial responses of a two-dimensional airfoil are shown in Fig. 1 for Mach numbers of 0.3, 0.5, and 0.8. The lift is plotted against the nondimensional time $S = 2VT/C$, where V is the freestream velocity, T is time, and C is the chord length. It is seen that the noncirculatory lift builds up instantaneously with the change in the angle of attack. Thereafter, the contribution caused by noncirculatory lift starts decaying while the circulatory lift starts building up. The noncirculatory lift decays within a few chord lengths of distance traveled and the total lift asymptotes toward the steady-state value corresponding to the effective angle of attack.

Table 1 shows the comparison of the lift values predicted by the analytical theories and the lift magnitudes obtained using the CFD method. The lift magnitudes at time $S = 0$ are compared with values predicted by the linear piston theory. The initial lift magnitudes are shown for two different time step sizes used for the unsteady time marching. Lift peak values increased and asymptotically reached about the values shown for $\Delta S = 10^{-5}$ as the time step size was decreased. The initial lift magnitudes predicted using linear piston theory are also shown for two methods: 1) one based on the freestream Mach number and 2) another based on the average initial Mach number over the airfoil surface. It is seen from Table 1 that the CFD calculated values for the smaller time step are in good agreement with the values calculated based on the average Mach number over the airfoil. The difference in peak magnitudes predicted by the two CFD results, however, do not affect the subsequent lift time history for practical applications since the rise to the peak magnitude occurs over a very small time, and after the peak magnitude is attained the time history curves converges to a single curve within a very short time period. The lift values at $S = 50$ are compared to the final values given by the linearized compressible theory. This is most likely because of the nonlinear effects captured by the CFD calculations.

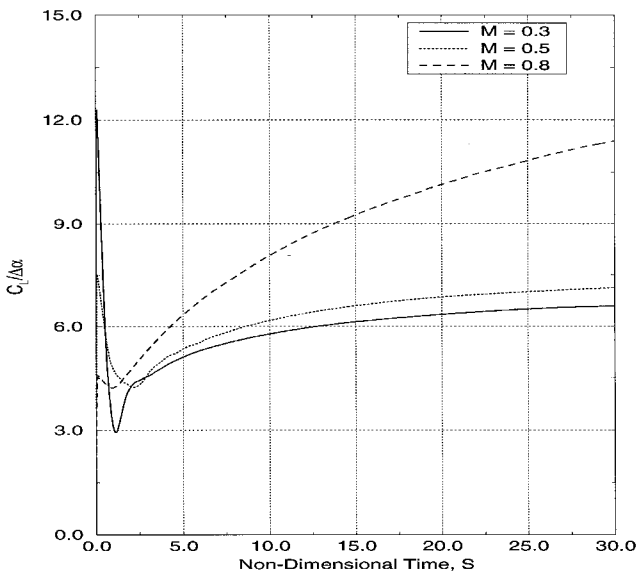

Fig. 1 Two-dimensional indicial lift response to a step change in the angle of attack (CFD).

The chordwise pressure distribution, being more local in character than the lift magnitude, provides another rigorous test of the accuracy of the method. The development of the flow after the indicial input is shown in Fig. 2, where the pressure distributions based on the linear compressible theory are also shown. Unfortunately, analytical pressure distributions can be computed for only a very short period after the motion begins. The interaction between the forward-moving wave from the trailing edge and the backward-moving wave from the leading edge does not allow for further theoretical analysis. Moreover, nonlinear effects in the transonic range are also not accounted for in the linear theory. It can be seen from the figures that for Mach numbers of 0.3 and 0.5 the pressure distributions calculated by CFD are in excellent agreement with the analytical pressure distributions. The progression of pressure waves from the leading edge and the trailing edge are captured accurately. The pressure distributions for a Mach number of 0.8 differ more significantly, quite expectedly, because of the neglect of transonic effects in the analytical pressure distributions. Thickness effects result in a slightly nonflat, noncirculatory response at all Mach numbers.

Perturbation pressure contours in the flowfield are shown in Fig. 3 for three successive values of time for $M = 0.5$. The perturbation pressures are obtained by subtracting the steady-state pressure from the current pressure to remove the thickness effects. The propagation of pressure waves, as indicated by the clustering of the pressure contours, can be easily observed in these figures. Since the forward- and backward-moving waves have speeds of $1 + M$ and $1 - M$, respectively, the plot for $S = 0.5$ shows the point where the two waves interact. As to be expected, these waves meet at 75% chord from the leading edge.

Three-Dimensional Indicial Response

Since the CFD method compares favorably with the analytical results for two-dimensional flow, one can proceed with some level of confidence to examine three-dimensional indicial responses of wings. In Fig. 4 indicial responses are shown for the wings of aspect ratio 5 and 10 at various spanwise locations for the same three Mach numbers as for the airfoil results. The two-dimensional indicial responses for a NACA 0012 airfoil are also superimposed on the plots. Since the chord length is the characteristic length for the flow, it is reasonable to expect flow for the two different aspect ratio wings to have similar behavior at the same chord distance from the tip. Therefore, results are shown for five different spanwise stations at the same chord distance from the tip for the two wings. In the figures d represents the distance in terms of chord length from the wing tip, and AR is the aspect ratio.

It is seen that the lift at $S = 0$ is the same for all spanwise locations for a given Mach number (the same as the two-di-

Table 1 Initial and final magnitudes of $C_L/\Delta\alpha$ for the two-dimensional indicial response to a step change in the angle of attack

	$S = 0$				$S = 50$	
	CFD		Piston theory			
Mach number	$\Delta S = 10^{-2}$	$\Delta S = 10^{-5}$	M_∞	M_{av}	CFD	Linear compressible theory
0.3	12.29	13.74	13.33	13.75	6.71	6.58
0.5	7.46	8.01	8.00	8.10	7.64	7.25
0.8	4.57	4.78	5.00	4.85	12.11	10.47

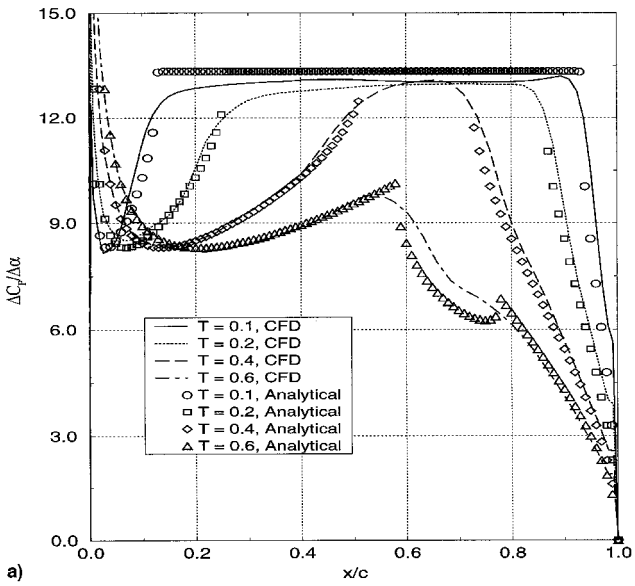

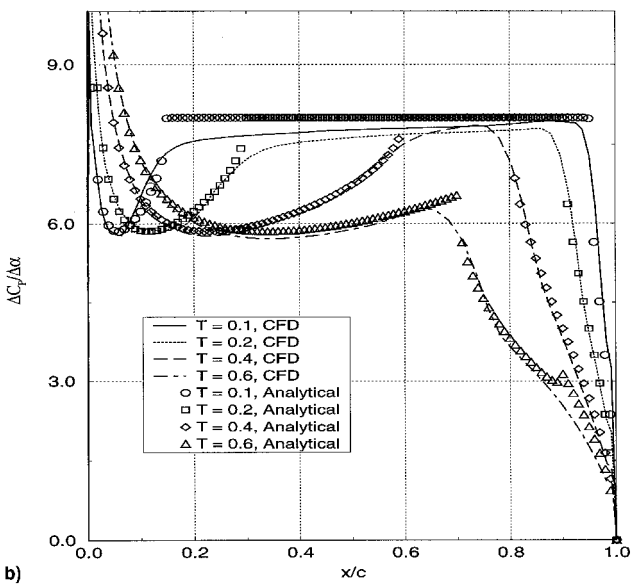

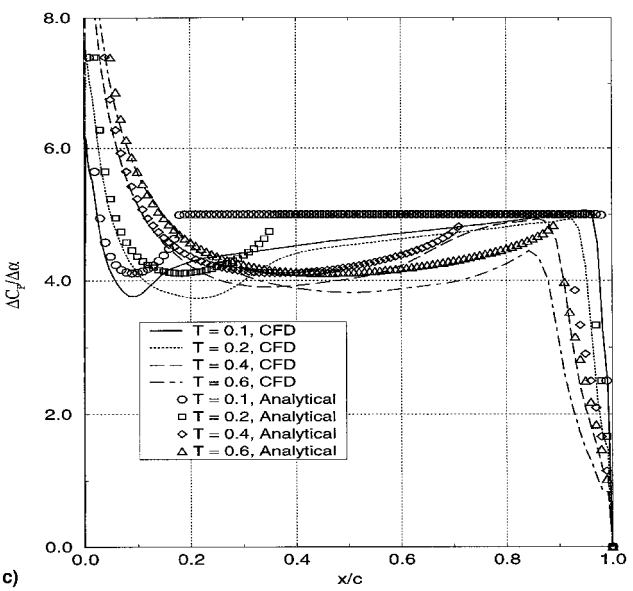

Fig. 2 Comparision of CFD and analytical solutions to two-dimensional indicial response to a step change in the angle of attack. M = a) 0.3, b) 0.5, and c) 0.8.

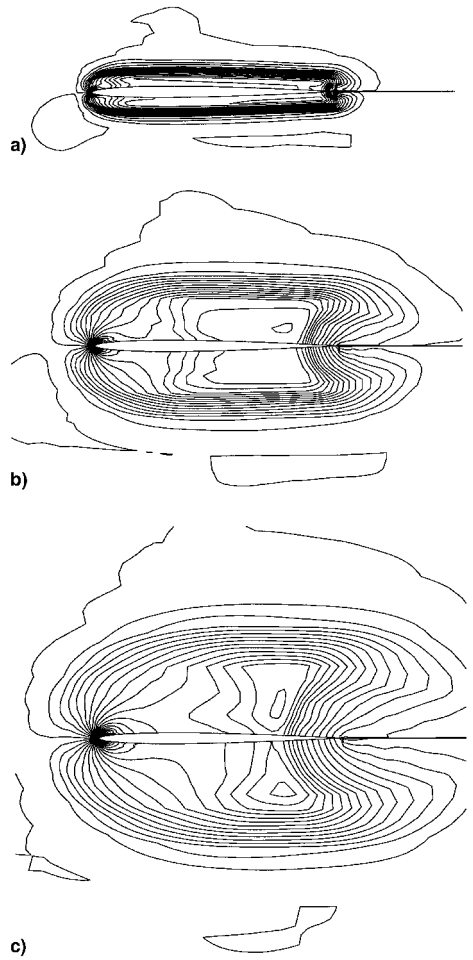

Fig. 3 Perturbation pressure contours for two-dimensional indicial response at M = 0.5 for NACA 0006 airfoil. S = a) 0.1, b) 0.3, and c) 0.5.

mensional value). This is consistent with the fact that the pressure disturbance caused by the impulsive motion of the wing is uniform over all of the surface, and it takes a finite time for the influence of the three-dimensional effects to be felt. For all of the cases, the initial calculated values of the lift are slightly lower than the value predicted by the two-dimensional linear piston theory. As time progresses, the various spanwise stations attain different steady-state values of lift. The steady-state lift reached is lower for the outboard stations. Sections closer to the wing tip are influenced more by the tip-relief effects than the sections further away from it, hence, the smaller magnitudes for the outer sections. The spanwise variation of the lift on the wing is nearly elliptical corresponding to steady state. In the intermediate time range, the lift is first seen to decrease with a minima occuring at different times at the various stations, followed by a gradual increase to the steady-state circulatory value. Fig. 5 shows the time history of the total wing lift. As expected, the lift magnitude for the wing of aspect ratio 10 is closer to the two-dimensional lift response. However, the shape of the lift time history curves are nearly identical in both cases, which suggests that a general parametric representation is possible by simply modifying the two-dimensional indicial response approximations.

Figure 6 shows the lift time history for small times after the indicial change in the angle of attack to highlight the rate of decay of the lift at various spanwise sections. It can be seen that immediately after the peak magnitude is reached the lift curves overlap for all span locations. However, as time increases, the lift history curves for outer sections begin to separate from the other inner sections. This departure of a curve

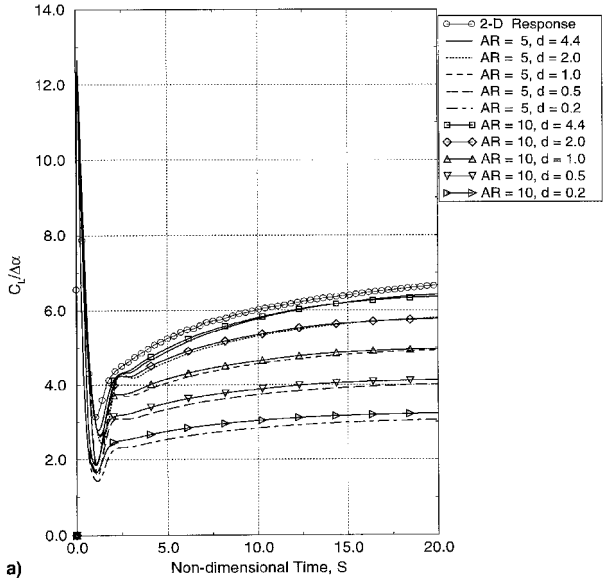

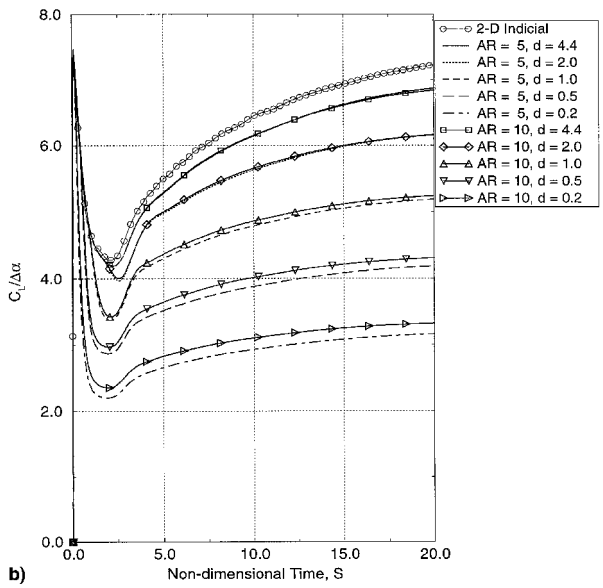

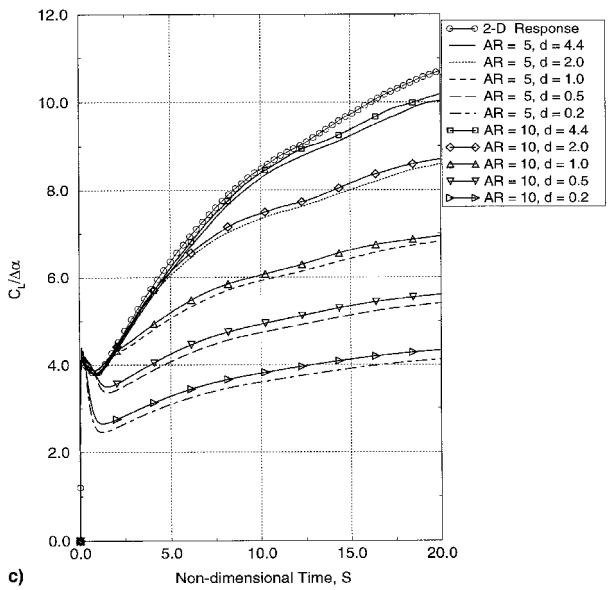

Fig. 4 Indicial response to a step change in the angle of attack for wings of aspect ratio 5 and 10 at various chord distances from the wing tip. M = a) 0.3, b) 0.5, and c) 0.8.

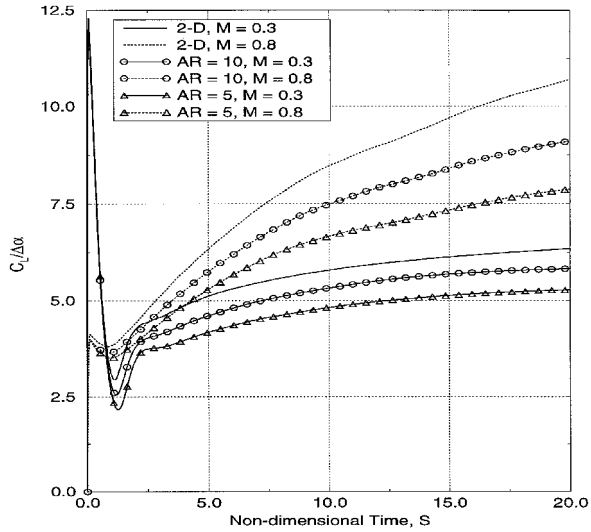

Fig. 5 Time history of total lift for three-dimensional indicial response for wings of aspect ratio 5 and 10 at various Mach numbers.

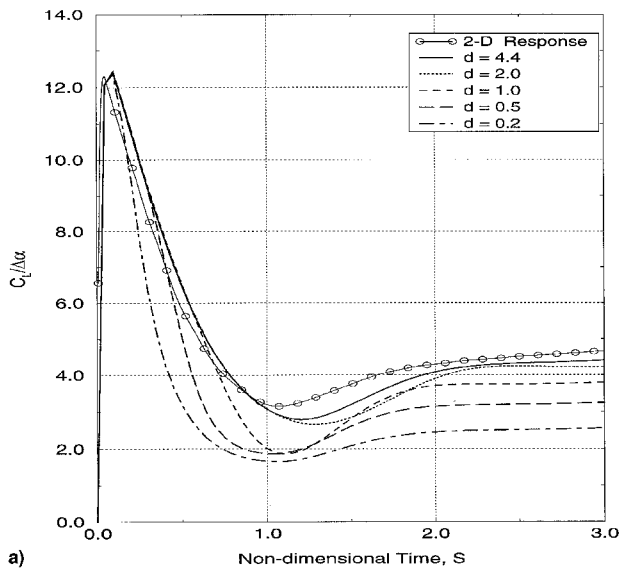

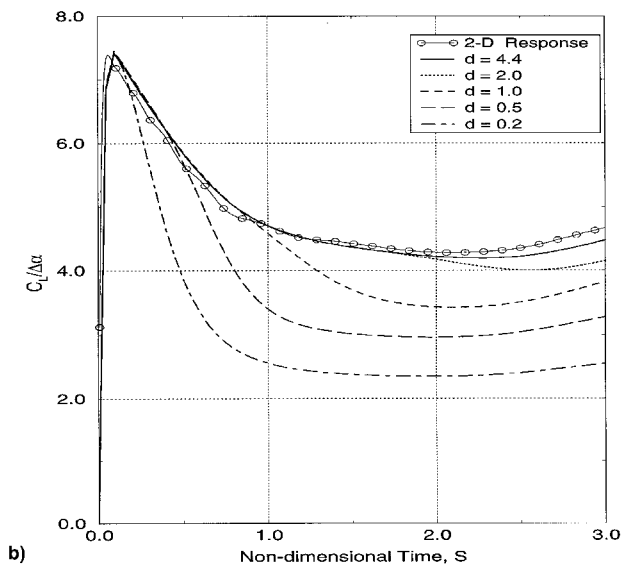

Fig. 6 Decay of the noncirculatory lift in three-dimensional indicial response for the wing of aspect ratio 10 at various span locations M = a) 0.3 and b) 0.5.

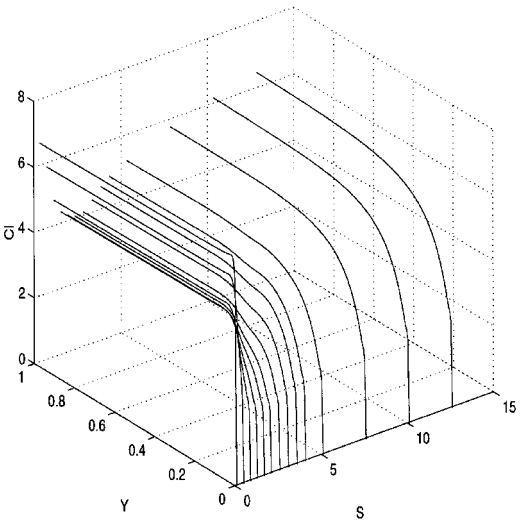

Fig. 7 Spanwise development of the flow at $M = 0.5$ for the indicial response of the wing of aspect ratio 10.

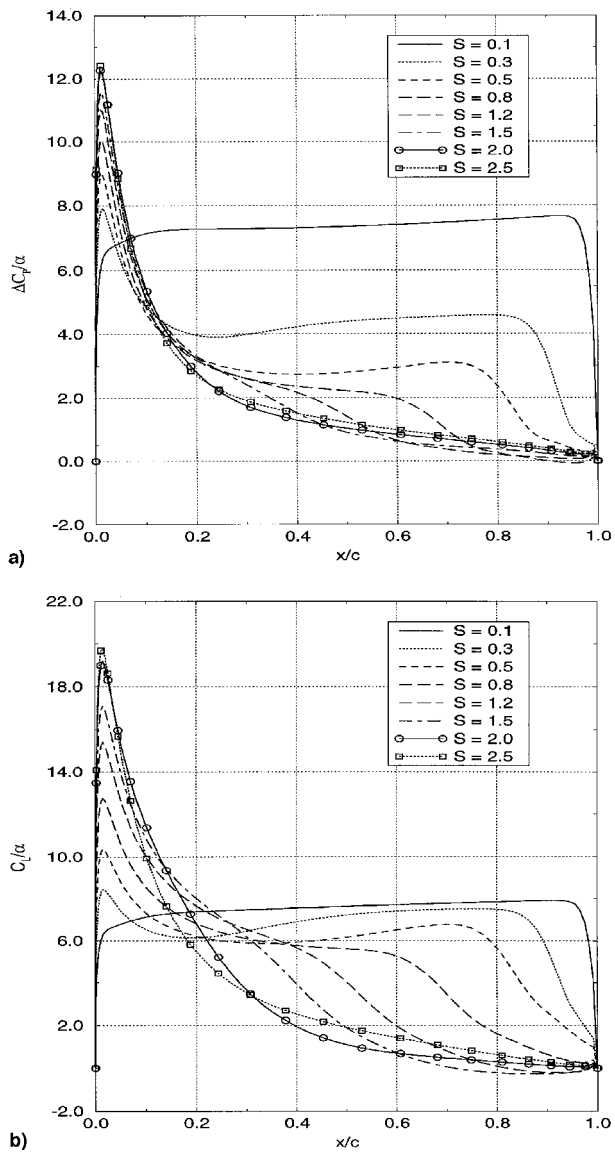

Fig. 8 Development of the flow for the indicial response of the wing of aspect ratio 10 at different span locations at $M = 0.5$. d = a) 0.2 and b) 1.0.

for a given section occurs when the three-dimensional effects propagating inward from the wing tip reach that section. The time of departure matches excellently with the time predicted assuming linear propagation of the three-dimensional effects at the characteristic velocity. For a M, the S for three-dimensional effects to influence a given section at a distance d from the wing tip is given by $d/2M$.

Curves of the lift time histories for the wings of different aspect ratios at the same nondimensional chord distance from the wing tip show that for low subsonic Mach numbers the lift times histories are almost identical for stations at a distance of more than 1 chord from the wing tip in both the noncirculatory and the circulatory load-dominated regions. This suggests the possibility of parametrization of the indicial response in terms of the distance from the tip in chords. For transonic Mach numbers there is a small difference between the two cases for the circulatory loads. The initial rates of decay at any given section located at equal nondimensional chord distance from the tip are the same for any given Mach number.

The development of lift from the initial noncirculatory lift to the final circulatory lift is shown in Fig. 7. It shows the spanwise variation of lift at various times for a Mach number of 0.5 and the wing of aspect ratio 10. The transformation of the lift distribution from being rectangular initially to elliptical at later times is clearly visible. Similarly, the chordwise variation of the pressure coefficient in the unsteady loading is shown in Fig. 8 for two spanwise stations on the same wing at $d = 0.2$ and $d = 1.0$. Figures 7 and 8 show the progressive development of a peak near the leading edge and a drop in the pressure coefficient magnitude over the aft region of the wing.

Figure 9 shows the time histories of the normalized lift coefficient at various spanwise locations for the wing of aspect ratio 10 at Mach number of 0.5. The lift coefficient is normalized by the steady-state lift coefficient magnitude at that section. It can be seen that the curves for different spanwise locations collapse onto a single curve for the later stages of the response. The time derivative of the curves is also the same for all of the sections during the decay period of the noncirculatory loading. This again suggests that the three-dimensional indicial response to a step change in the angle of attack at a given Mach number can be accurately expressed using the two-dimensional lift response at the same Mach number and a few parameters to account for the three-dimensional effects.

To gain more insight into the flow features, pressure contour plots are shown for the pressure difference between the top

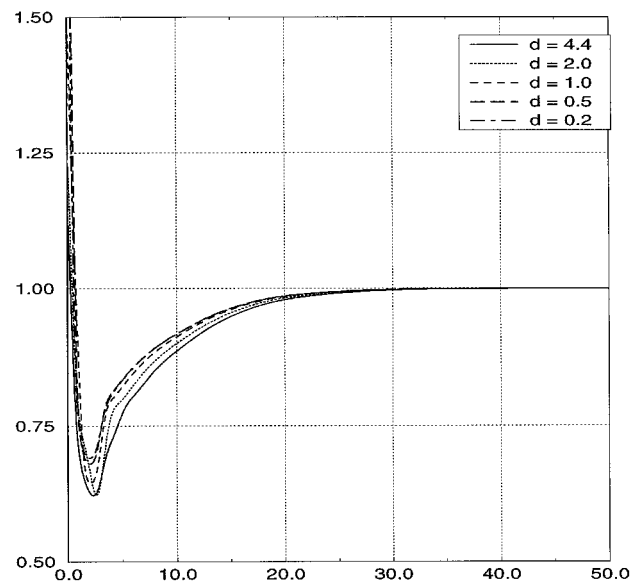

Fig. 9 Time history of lift coefficient normalized by the steady-state magnitude for the three-dimensional indicial lift response at $M = 0.5$.

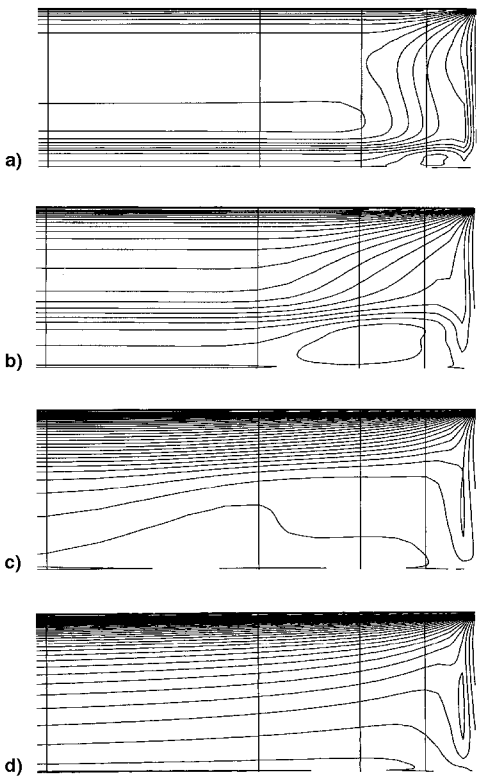

Fig. 10 Perturbation pressure contours for the indicial response of the wing of aspect ratio 10 at $M = 0.5$. S = a) 0.2, b) 0.4, c) 0.8, and d) 2.0.

and bottom surface in Fig. 10 at four representative times. Thus, the plotted pressure fields are caused entirely by the impulsive change in the angle of attack. Only the outboard portions of the wing, which have significant three-dimensional effects, are shown in the figures. The leading edge of the wing is on the top. Vertical lines on the plot mark the locations of the four outer stations for which lift histories are shown in Fig. 10.

The transition of aerodynamic loads over the wing from initial noncirculatory loads occur because of two simultaneously occuring processes. There is a decay of noncirculatory loads, similar to the two-dimensional indicial response shown earlier, caused by the propagation of pressure waves from the trailing edge. This can be seen for the pressure contour plots at S = 0.2 and 0.4. Pressure contours are parallel to the wing edges over most of the wing in Fig. 10, which suggests that the loading is uniform along the spanwise direction. Another process taking place in the three-dimensional indicial response is the propagation of tip relief effects from the wing tip. The portion of the wing near the trailing-edge tip is affected by both of these waves, in which the combined effect of these two processes is to produce a region of low-pressure coefficient that moves inward from the trailing-edge tip of the wing. It can also be observed that by the time $S = 2.0$ the pressure contours attain the pattern corresponding to steady state.

Conclusions

For the first time, the indicial response of a wing to a step change in angle of attack is calculated directly using a CFD method. The lift histories and pressure contour plots are shown to explain the characteristics of the three-dimensional indicial response. It is found that CFD methods can accurately calculate the indicial response and are very useful tools in developing and validating approximations to the indicial response functions. The nondimensional chord distance from the wing tip is shown to be an important parameter in forming the approximations of the indicial response for the wings of different aspect ratios. Similar calculations can be performed to develop indicial responses for wings of arbitrary planform.

Acknowledgments

This work was supported by NASA Research Grant NAG-1-1655 with Kenneth Brentner as the Contract Monitor, it was supported as well by National Rotorcraft Technology Center Grant NCC-2944. All calculations were performed on a DEC Alpha 600 5/333 workstation with funding from the University of Maryland Graduate Research Equipment Board. The authors would like to acknowledge J. Gordan Leishman for his many helpful discussions.

References

[1]Bisplinghoff, R. L., Ashley, H., and Halfman, R. L., *Aeroelasticity*, Addison–Wesley, Reading, MA, 1955.

[2]Lomax, H., "Indicial Aerodynamics," *AGARD Manual of Aeroelasticity*, Pt. 2, Nov. 1960, Chap. 6.

[3]Leishman, J. G., "Indicial Lift Approximations for Two-Dimensional Subsonic Flow as Obtained from Oscillatory Measurements," *Journal of Aircraft*, Vol. 30, No. 3, 1993, pp. 340–351.

[4]Leishman, J. G., "Validation of Approximate Indicial Aerodynamic Functions for Two-Dimensional Subsonic Flow," *Journal of Aircraft*, Vol. 25, No. 10, 1988, pp. 914–922.

[5]Lesieuture, D. J., Reisenthel, P. H., and Dillenius, M. F. E., "A Practical Approach for Calculating Aerodynamic Indicial Functions with a Navier-Stokes Solver," AIAA Paper 94-0059, Jan. 1994.

[6]Srinivasan, G. R., and Baeder, J. D., "TURNS: A Free Wake Euler/Navier–Stokes Numerical Method for Helicopter Rotors," *AIAA Journal*, Vol. 31, No. 5, 1993, pp. 2371–2378.

[7]Parameswaran, V. and Baeder, J. D., "Indicial Aerodynamics in Compressible Flow—Direct Computational Fluid Dynamic Calculations," *Journal of Aircraft*, Vol. 34, No. 1, 1997, pp. 131–133.

[8]Khanna, H., and Baeder, J. D., "Coupled Wake/CFD Solutions for Rotors in Hover," 52nd Annual Forum of the American Helicopter Society, Washington DC, June 1996.